J|A|C|S
ARTICLES
Published on Web 04/22/2006

^{17}O Solid-State NMR Spectroscopic Studies of the Involvement of Water Vapor in Molecular Sieve Formation by Dry-Gel Conversion

Banghao Chen and Yining Huang*

Contribution from the Department of Chemistry, The University of Western Ontario, London, Ontario, Canada N6A 5B7

Received January 14, 2006; E-mail: yhuang@uwo.ca

Abstract: Dry-gel conversion is a relatively new approach for molecular sieve synthesis. This method potentially has several advantages over the traditional hydrothermal synthesis and can be used to prepare molecular sieves with certain unique properties. The technique involves treating the predried reactive gel powder with water vapor at elevated temperature and pressure. The role of water vapor in this apparent solid transformation is, however, not clear. In this work, we directly monitored the involvement of ^{17}O-enriched water vapor in crystallization of $AlPO_4$-11 (an aluminophosphate-based molecular sieve) by ^{17}O solid-state NMR spectroscopy. In addition to ^{17}O magic-angle spinning technique, several dipolar-coupling based double-resonance methods including $^{17}O\{^{27}Al\}$, $^{17}O\{^{31}P\}$ rotational-echo double-resonance, $^{17}O \rightarrow {}^{31}P$ and $^{1}H \rightarrow {}^{17}O$ cross polarization techniques were used for spectral editing to select different ^{17}O species. The results show that water from the vapor phase slowly exchanges with water molecules strongly bound to the AlPO intermediates first. Then ^{17}O atoms are gradually incorporated in both P−O−H and P−O−Al units in the layered intermediate. There are three different P sites in $AlPO_4$-11. Interestingly, during the transformation from the layered intermediate to $AlPO_4$-11, the ^{17}O atoms prefer to bond to the P(2) and P(3), but not to P(1). The absence of ^{17}O atoms in the first coordination sphere of P(1) site suggests that some building units such as joint four- and six-membered rings involving hydrogen bonding with structure-directing agents are common in both layered intermediate and $AlPO_4$-11 and they are not affected by the transformation from the layered phase to the $AlPO_4$-11 framework.

Introduction

Zeolite molecular sieves are three-dimensional aluminosilicate-based framework materials containing regular systems of channels and cavities with molecular dimensions. They are extensively used in industry for ion-exchange, separation, and in particular, catalysis.[1] Another important type of molecular sieve is aluminophosphate ($AlPO_4$)-based material.[2] The $AlPO_4$-based molecular sieves exhibit distinct molecular sieving characteristics and can be made catalytically active by introducing Si and metal ions into the framework.

Zeolites and $AlPO_4$s are usually prepared by hydrothermal synthesis. In recent years, a new approach, namely dry-gel conversion (DGC), has been developed.[3] The technique involves treating predried reactive gel powder in vapor at elevated temperature and pressure. It can be further classified into two related methods: steam-assisted conversion (SAC) and vapor-phase transport (VPT).[3c,4] In the SAC approach, prior to heating, the predried gel powder containing organic structure-directing agents (SDAs) are physically separated from a very small amount of pure water in an autoclave (Scheme 1), and the dry-gel powder is converted to a zeolite in steam upon heating. The VPT method is similar to SAC except that the SDA is not contained in the initial dry-gel. Instead of pure water, a small amount of aqueous solution containing SDA is placed at the bottom of the autoclave, and SDA molecules are brought in contact with the dry-gel powder through the vapor phase. Recently, these methods have received much attention since they are particularly effective in the preparation of nanozeolite crystals with uniform particle size,[4a] zeolite membranes on a variety of supports,[5] and molecular sieves with a high metal content.[6] Other potential advantages over the conventional hydrothermal synthesis include minimization of waste disposal, reduction of energy consumption and reactor volume, rapid crystallization with a high yield, and lowering the cost by reducing the use of SDAs.[3a,7]

To effectively use the DGC techniques for molecular sieve synthesis it is crucial to understand the crystallization processes

(1) Van Bekkum, H.; Flanigen, E. M.; Jacobs, P. A.; Jansen, J. C., Eds. *Introduction to Zeolite Science and Practice*, 2nd ed., Elsevier: Amsterdam, 2001.
(2) Wilson, S. T.; Lok, B. M.; Messina, C. A.; Cannan, T. R.; Flanigen, E. M. *J. Am. Chem. Soc.* **1982**, *104*, 1146−1147.
(3) (a) Xu, W.; Dong, J.; Li, J.; Li, J.; Wu, F. *J. Chem. Soc., Chem. Commun.* **1990**, 755−756. (b) Kim, M. H.; Li, H. X.; Davis, M. E. *Microporous Mater.* **1993**, *1*, 191−200. (c) Rao, P. R. H. P.; Matsukata, M. *Chem. Commun.* **1996**, 1441−1442.
(4) (a) Rao, P. R. H. P.; Ueyama, K. Matsukata, M. *Appl. Catal.* **1998**, *166*, 97−103. (b) Tatsumi, T.; Xia, Q.; Jappar, N. *Chem. Lett.* **1997**, 677−678. (c) Bandyopadhyay, R.; Kubota, Y.; Ogawa, M.; Sugimoto, N.; Fukushima, Y.; Sugi, Y. *Chem. Lett.* **2000**, 300−301.
(5) (a) Matsukata, M.; Kikuchi, E. *Bull. Chem. Soc. Jpn.* **1997**, *70*, 2341−2356. (b) Dong, W. Y.; Long, Y. C. *Chem. Commun.* **2000**, 1067−1068.
(6) Arnold, A.; Hunger, M.; Weitkamp, J. *Microporous Mesoporous Mater.* **2004**, *67*, 205−213.

10.1021/ja060286t CCC: $33.50

Scheme 1. Schematic Diagram of the Reaction Vessel Used for Synthesis of $AlPO_4$-11 by Steam-Assisted Conversion (SAC)

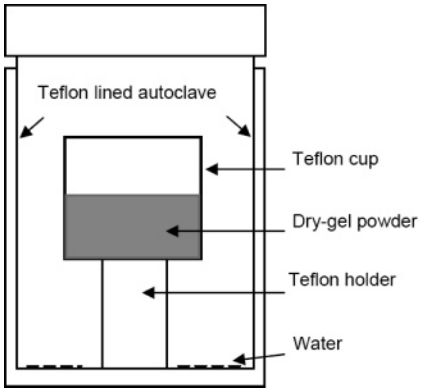

Scheme 2. Structure of $AlPO_4$-11

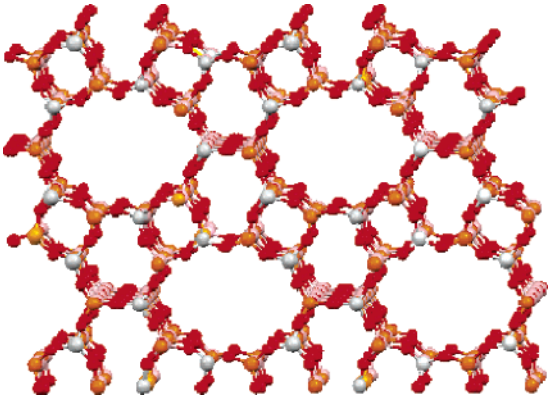

under DGC conditions. Since transformation from initial dry-gel powder to zeolitic framework is mediated by steam, understanding the role of water vapor is fundamentally important. Despite several extensive and high-quality studies that focused on the issue,[3,8] there exist few direct observations on how water is involved in crystallization at an atomic level. ^{17}O solid-state NMR spectroscopy has been proven to be a powerful tool for characterization of oxygen sites in various molecular sieve frameworks.[9−15] Although solid-state ^{29}Si, ^{27}Al, ^{13}C, ^{71}Ga, and ^{1}H NMR spectroscopies have been utilized for investigating the crystallization under DGC conditions,[3b,c,4a,6,7,8b,c] ^{17}O NMR has not been employed to examine dry-gel synthesis. In this work, we provide direct information on the involvement of water during crystallization of $AlPO_4$-11, an $AlPO_4$-based molecular sieve with AEL structure (Scheme 2) under SAC conditions. In particular, we prepared a series of intermediates by placing initial dry-gel prepared from normal water ($H_2{}^{16}O$) in a Teflon cup and a small amount of ^{17}O-enriched water at the bottom of each autoclave as the source of vapor. The autoclaves were then heated at 448 K for different lengths of time. ^{17}O solid-state NMR was used to directly monitor the ^{17}O incorporation at various stages of the crystallization. Since the initial dry-gel powder is physically separated from $H_2{}^{17}O$ before heating, any ^{17}O signal in the solids must result from the reaction with $H_2{}^{17}O$ vapor. We demonstrate that a combination of ^{17}O magic-angle spinning (MAS) and several dipolar-coupling-based double-resonance techniques such as $^{17}O\{^{27}Al\}$, $^{17}O\{^{31}P\}$ rotational-echo double-resonance (REDOR), $^{17}O \rightarrow {}^{31}P$ and $^{1}H \rightarrow {}^{17}O$ cross polarization (CP) is a sensitive probe for information on crystallization of molecular sieves by DGC.

Experimental Section

Sample Preparation. The aluminum and phosphorus sources were $Al(OH)_3$ (50% Al_2O_3) and 85% H_3PO_4. Di-*n*-propylamine (DPA) was used as SDA. All the chemicals were purchased from Aldrich Chemical Co. The composition for the initial dry-gel ($Al_2O_3/P_2O_5/Pr_2NH/H_2O$) is 1:1:1:40. A typical procedure[8c] for the preparation of SAC dry-gel powder is the following: an appropriate amount of aluminum hydroxide was mixed with distilled normal water ($H_2{}^{16}O$), and the mixture was stirred at room temperature for 30 min followed by the dropwise addition of 85% phosphoric acid with continuous stirring. DPA was then added with continuous stirring. This wet gel was dried at 353 K with constant stirring to allow evaporation of water until white solids formed. The solid sample was then ground into a fine powder which will be hereafter referred to as the initial dry-gel. We prepared a series of intermediates by typically placing 1.0 g of the above initial dry-gel powder into a series of small Teflon cups. Each cup was placed in a Teflon-lined autoclave (volume: 23 mL) with 0.3 mL of 35% ^{17}O-enriched water (Cambridge Isotope Laboratories, Inc.) at the bottom (Scheme 1). The crystallization was then carried out at 448 K in an oven. The autoclaves were taken out of the oven at different times, and the reactions were quenched in cold water. The dried solid samples were kept in tightly sealed glass vials for analysis.

NMR Measurements. All the NMR experiments were carried out on a Varian/Chemagnetics Infinityplus 400 WB spectrometer equipped with three rf channels operating at the field strength of 9.4 T. The Larmor frequencies of ^{1}H, ^{17}O, ^{31}P, and ^{27}Al were 399.9, 54.2, 161.6, and 104.1 MHz, respectively. The ^{17}O MAS spectra were acquired by using a Varian/Chemagnetics 4-mm T3 triple-tuned MAS probe, using a small pulse angle (less than 15°) to ensure the quantitative spectra with a recycle delay of 1 s. The spinning speed for simple MAS experiments was in the range 12−15 kHz. $^{1}H \rightarrow {}^{17}O$ cross polarization spectra were also collected by using the same 4-mm probe. The Hartmann−Hahn matching condition was set on ^{17}O-enriched $Mg(OH)_2$ with a contact time of 100 μs, and the recycle delay was 5 s.[16] ^{17}O

(7) Bandyopadhyay, R.; Kubota, Y.; Sugimoto, N.; Fukushima, Y.; Sugi, Y. *Microporous Mesoporous Mater.* **1999**, *32*, 81−91.
(8) (a) Matsukata, M.; Ogura, M.; Osaki, T.; Rao, P. R. H. P.; Nomura, M.; Kikuchi, E. *Top. Catal.* **1999**, *9*, 77−92. (b) Arnold, A.; Steuernagel S.; Hunger, M.; Weitkamp, J.; *Microporous Mesoporous Mater.* **2003**, *62*, 97−106. (c) Rajib, B.; Mahuya, B.; Kubota, Y.; Sugi, Y. *J. Porous Mater.* **2002**, *9*, 83−95. (d) Cundy, C. S.; Cox, P. A. *Microporous Mesoporous Mater.* **2005**, *82*, 1−78.
(9) Mackenzie, K. J. D.; Smith, M. E. *Multinuclear Solid-state NMR of Inorganic Materials*, Pergamon: Amsterdam, 2002; pp 333−395.
(10) (a) Timken, H. K. C.; Turner, G. L.; Gilson, J. P.; Welsh, L. B.; Oldfield, E. *J. Am. Chem. Soc.* **1986**, *108*, 7231−7235. (b) Timken, H. K. C.; Janes, N.; Turner, G. L.; Lambert, S. L.; Welsh, L. B.; Oldfield, E. *J. Am. Chem. Soc.* **1986**, *108*, 7236−7241. (c) Yang, S.; Park, K. D.; Oldfield, E. *J. Am. Chem. Soc.* **1989**, *111*, 7278−7279.
(11) Ernst, H.; Freude, D.; Kanellopoulos, J.; Loeser, T.; Prochnow, D.; Schneider, D. *Stud. Surf. Sci. Catal.* **2004**, *154*, 1173−1179.
(12) (a) Peng, L.; Liu, Y.; Kim, N.; Readman, J. E.; Grey, C. P. *Nat. Mater.* **2005**, *4*, 216−219. (b) Readman, J. E.; Grey, C. P.; Ziliox, M.; Bull, L. M.; Samoson, A. *Solid State NMR* **2004**, *26*, 153−159. (c) Readman, J. E.; Kim, N.; Ziliox, M.; Grey, C. P. *Chem. Commun.* **2002**, *23*, 2808−2809.
(13) (a) Neuhoff, P. S.; Zhao, P.; Stebbins, J. F. *Microporous Mesoporous Mater.* **2002**, *55*, 239−251. (b) Zhao, P.; Neuhoff, P. S.; Stebbins, J. F. *Chem. Phys. Lett.* **2001**, *344*, 325−332. (c) Xu, Z.; Stebbins, J. F. *Geochim. Cosmochim. Acta* **1998**, *62*, 1803−1809.
(14) (a) Loeser, T.; Freude, D.; Mabande, G. T. P.; Schwieger, W. *Chem. Phys. Lett.* **2003**, *370*, 32−38. (b) Bull, L. M.; Cheetham, A. K.; Anupold, T.; Reinhold: A.; Samoson, A.; Sauer, J.; Bussemer, B.; Lee, Y.; Gann, S.; Shore, J.; Pines, A.; Dupree, R. *J. Am. Chem. Soc.* **1998**, *120*, 3510−3511. (c) Freude, D.; Loeser, T.; Michel, D.; Pingel, U., Prochnow, D. *Solid State NMR* **2001**, *20*, 46−60. (d) Pingel, U. T.; Amoureux, J. P.; Anupold, T.; Bauer, F.; Ernst, H.; Fernandez, C.; Freude, D.; Samoson, A. *Chem. Phys. Lett.* **1998**, *294*, 345−350. (e) Amoureux, J. P.; Bauer, F.; Ernst, H.; Fernandez, C.; Freude, D.; Michel, D.; Pingel, U. T.; *Chem. Phys. Lett.* **1998**, *285*, 10−14.
(15) (a) Vermillion, K. E.; Florian, P.; Grandinetti P. J. *J. Chem. Phys.* **1998**, *108*, 7274−7285. (b) Clark, T. M.; Grandinetti, P. J.; Florian, P.; Stebbins, J. F. *J. Phys. Chem. B* **2001**, *105*, 49, 12257−12265. (c) Profeta, M.; Mauri, F.; Pickard, C. J. *J. Am. Chem. Soc.* **2003**, *125*, 541−548. (d) Gervais, C.; Profeta, M.; Babonneuau, F.; Pickard, C. J.; Mauri, F. *J. Phys. Chem. B* **2004**, *108*, 13249−13253.

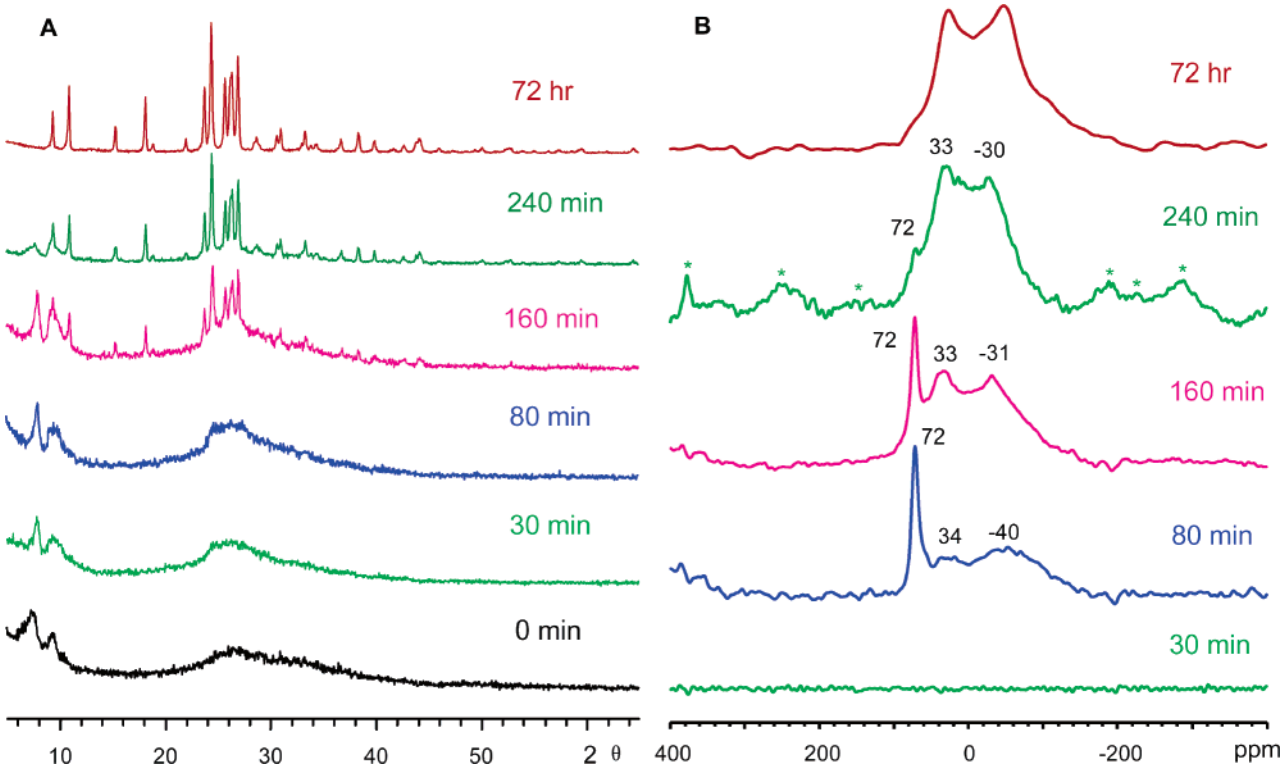

Figure 1. (A) Powder XRD patterns and (B) ^{17}O MAS NMR spectra of selected dry-gel samples. Asterisks indicate spinning sidebands.

static spectra were obtained by using a spin−echo sequence[17] with a Varian/Chemagnetics 5-mm wideline static double-tuned probe. The external reference for ^{17}O chemical shift was 0.1% ^{17}O-enriched water.

The REDOR experiment[18] is a rotor synchronized double-resonance MAS technique designed to probe the heteronuclear dipolar interactions. This technique involves two experiments with the first one being a normal spin−echo experiment on observing spin as a control experiment. In the second REDOR experiment, during the spin−echo, a number of 180° pulses are applied to dephasing nucleus. The echo intensity of the REDOR experiment will decrease due to nonzero average of dipolar coupling compared to the normal echo without 180° dephasing pulses. The REDOR difference spectrum (ΔS) is obtained by subtracting the REDOR spectrum (S) from the control spectrum (S_0) and indicates dipolar coupling. Since most the samples examined were obtained in the early stages of the crystallization, the level of ^{17}O-enrichment for various sites is very low. Therefore, to acquire REDOR difference spectra with a good signal-to-noise ratio in a reasonable period of time, a large sample volume is necessary. For this reason, a Varian/Chemagnetics 7.5-mm T3 triple-tuned MAS probe was used. The detailed spectrometer conditions for ^{17}O{^{27}Al} and ^{17}O{^{31}P} REDOR experiments are given in the corresponding figure captions. ^{17}O 3QMAS experiments were also attempted. Unfortunately, no meaningful spectrum could be obtained within a reasonable period of time, presumably due to the low level of ^{17}O exchange.

The same T3 7.5-mm probe was also employed for one-pulse ^{31}P and ^{27}Al MAS, ^{1}H → ^{31}P and ^{17}O → ^{31}P CP experiments. The spinning speed was typically at 6−7 kHz. For simple ^{31}P MAS experiments, the pulse length of 3 μs was used, corresponding to a nominal 90° pulse length of 10 μs. The rf field for ^{1}H decoupling was approximately 60 kHz, and the pulse delay was 120 s. The ^{27}Al MAS spectra were acquired by using a conventional one-pulse sequence with a very short rf pulse of 1 μs, which corresponds to a selective 90° pulse (central transition only) of 12 μs. The pulse delay was 0.2 s. Shift referencing was compared to 85% H_3PO_4, 1 M $Al(NO_3)_3$ (aq) for ^{31}P and ^{27}Al, respectively. The ^{17}O → ^{31}P cross polarization is also a technique based on dipolar interaction. Because ^{17}O ($I = 5/2$) is a quadrupolar nucleus, cross polarization is complicated since the spin-locking efficiency is affected by several factors.[19] The optimized strength of the ^{17}O spin-locking field is 24 kHz, corresponding to an ^{17}O 90° pulse length of 10.4 μs measured for the central transition. The spinning rate was 6.5 kHz, and the pulse delay was 0.5 s. For ^{1}H → ^{31}P cross polarization experiments, the ^{1}H 90° pulse length was 6 μs, and the Hartmann−Hahn condition was determined using $(NH_4)H_2PO_4$. A repetition time of 5 s was used. All NMR measurements were performed at room temperature. Quadrupolar parameters of various ^{17}O sites were extracted from simulations of the ^{17}O NMR spectra by using the WSOLIDS software package provided by Prof. Wasylishen (University of Alberta).

Powder X-ray diffraction patterns were recorded on a Rigaku diffractometer using Co Kα radiation (λ = 1.7902 Å).

Results and Discussion

The powder X-ray diffraction (XRD) patterns of selected samples were obtained to follow the evaluation of the long-range ordering as a function of crystallization time (Figure 1A). The XRD pattern of the initial dry-gel powder without SAC treatment contains two low-angle reflections, indicating a layered phase with some degree of long-range ordering. The pattern also shows the coexistence of an amorphous phase. After treating the initial dry-gel for 160 min, the reflections due to $AlPO_4$-11 starts appearing. Using quantitative ^{31}P MAS NMR, we have shown that upon heating the amorphous material is quickly converted to the layered material and the layered structure

(16) Walter, T. H.; Turner, G. L.; Oldfield, E. *J. Magn. Reson.* **1988**, *76*, 106−120.
(17) Kunwar, A. C.; Turner, G. L.; Oldfield, E. *J. Magn. Reson.* **1986**, *69*, 124−127.
(18) Gullion, T.; Schaefer, J. *J. Magn. Reson.* **1989**, *81*, 196−200.
(19) Vega, A. J. *Solid State NMR* **1992**, *1*, 17−32.

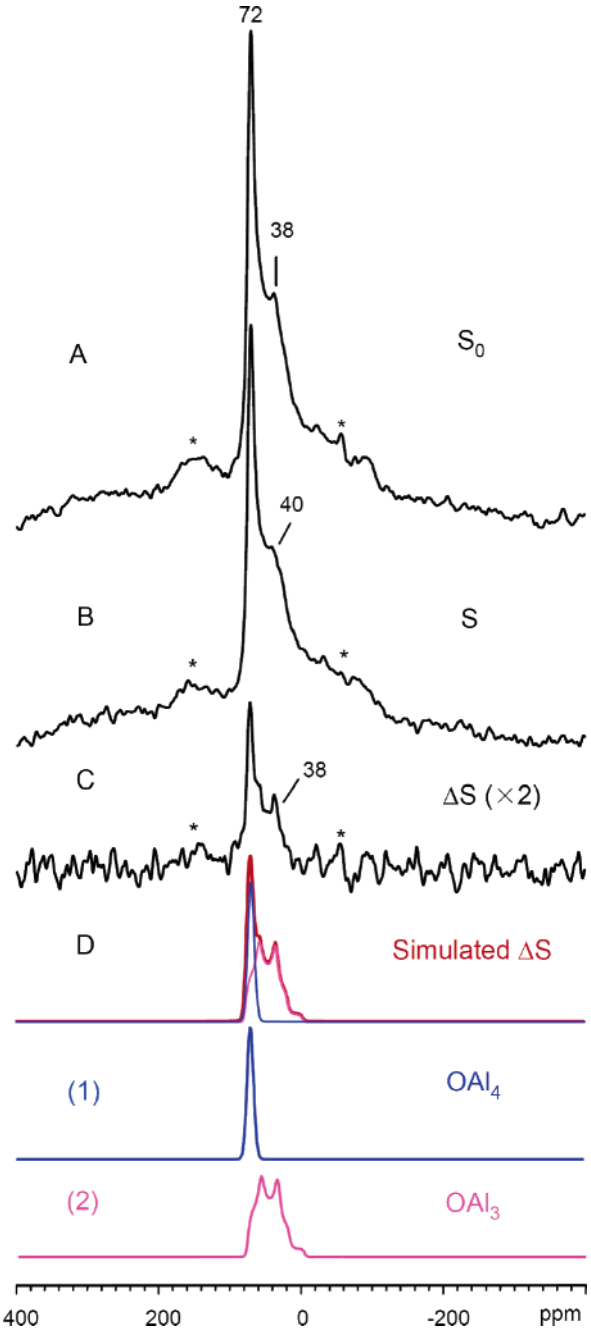

Figure 2. $^{17}O\{^{27}Al\}$ REDOR spectra of the dry-gel sample heated for 80 min. Eight rotor cycle periods were applied with a spinning rate at 7 kHz ± 2 Hz. A total of 125,984 scans were acquired with a recycle time of 0.5 s. The total experimental time was 35 h. (A) ^{17}O spin−echo (S_0); (B) REDOR (S); and (C) REDOR difference (ΔS) spectra. Asterisks indicate spinning sidebands. (D) Simulated REDOR difference spectrum using two components in a 1:2.3 ratio: (1) $C_q = 1.4$ MHz, $\eta = 0$, $\delta_{iso} = 74$ ppm, 230 Hz line broadening. (2) $C_q = 4.0$ MHz, $\eta = 0.4$, $\delta_{iso} = 80$ ppm, 190 Hz line broadening.

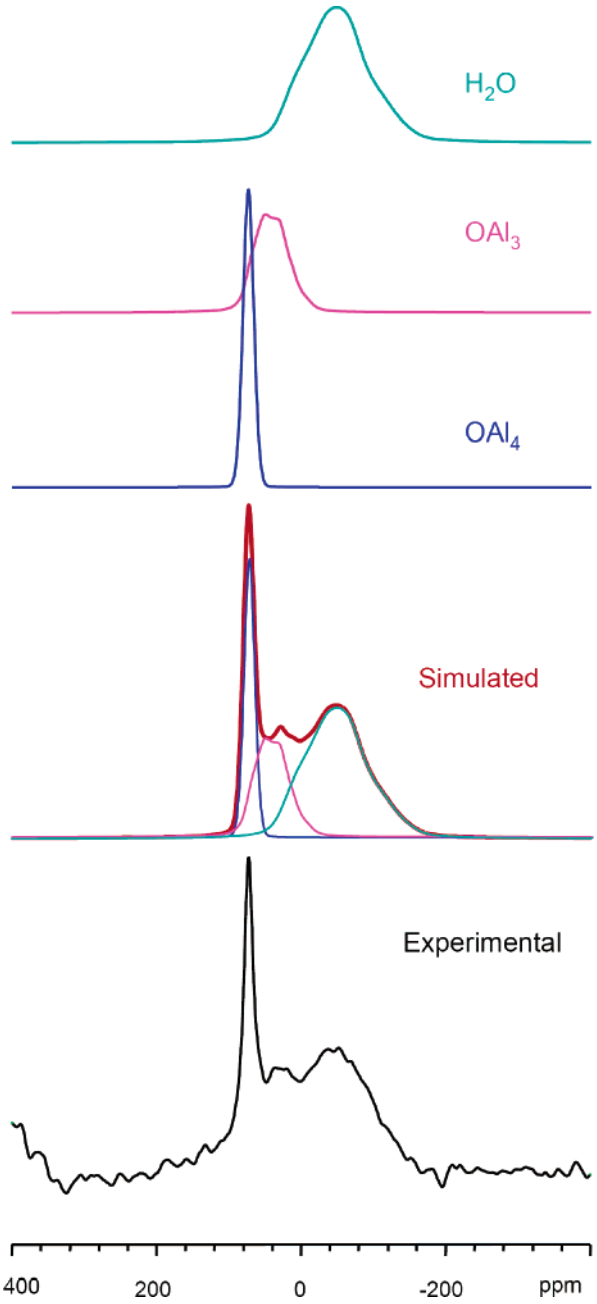

Figure 3. Simulation of ^{17}O MAS NMR spectrum of 80-min dry-gel sample. The quadrupolar parameters used for fitting the data are listed in Table 1.

gradually transforms into $AlPO_4$-11 (more detailed study of crystallization of $AlPO_4$-11 by dry-gel conversion will be presented in a subsequent publication).[20] The pattern of the sample heated for 72 h only contains the reflections of $AlPO_4$-11, implying that the dry-gel powder has been completely converted to highly crystalline $AlPO_4$-11.

The selected ^{17}O MAS spectra are shown in Figure 1B. No ^{17}O signal was observed in the MAS spectrum of the initial dry-gel sample heated for 30 min, indicating that ^{17}O has not been incorporated into any solid-state species. TGA data (not shown) indicate the initial dry-gel powder prior to the SAC treatment contains about 15% water. Observing no ^{17}O resonance during the first 30 min of heating implies that these water molecules are tightly bound to the solid species and have not exchanged with the ^{17}O-enriched water in vapor.

For the 80-min sample a sharp ^{17}O resonance at +72 ppm and several very broad overlapping signals with two broad maxima at around +34 and −40 ppm were observed in the ^{17}O MAS spectrum. Although the MAS spectrum clearly shows the existence of multiple oxygen sites, the severe peak overlapping coupled with the broadness of the resonances precludes the detailed spectral assignments. To distinguish different oxygen

(20) Chen, B.; Huang, Y. Manuscript in preparation.

Table 1. ^{17}O NMR Parameters Obtained from the Simulation of Selected ^{17}O NMR Spectra[a]

		this work				literature			
sample	site	C_q (e^2qQ/h) MHz	η	δ_{iso} ppm	intensity %	C_q (e^2qQ/h) MHz	η	δ_{iso} ppm	ref
80-min (MAS)	OAl_4	1.2 (0.1)	0.00 (0.01)	76 (1)	20	1.2	-	72	22
	OAl_3	4.2 (0.2)	0.46 (0.01)	79 (5)	22	4.0	0.6	79	22
	H_2O	5.8 (0.5)	0.62 (0.03)	27 (8)	58	~7	0.2	16−30	13a
160-min (MAS)	OAl_4	1.2 (0.1)	0.00 (0.01)	76 (1)	13				
	OAl_3	4.2 (0.3)	0.46 (0.02)	79 (3)	9				
	H_2O	5.7 (0.3)	0.62 (0.06)	30 (3)	45				
	Al−O−P	5.7 (0.2)	0.00 (0.02)	65 (1)	21	5.7	0	63	10b
	P−O−H	5.0 (0.2)	0.55 (0.03)	95 (5)	12	~5.1	0.55	93	23
72 h (MAS)	Al−O−P	6.0 (0.3)	0.00 (0.03)	68 (2)	79				
	H_2O	7.0 (0.4)	0.00 (0.05)	12 (3)	21				
72 h (Static)	Al−O−P	6.5 (0.2)	0.12 (0.03)	75 (2)	100	6.4	0	67	10b

[a] Note: the errors associated with C_q, η, and δ_{iso} are indicated in parentheses.

chemical environments and select possible Al−O and P−O connectivities, we further carried out $^{17}O\{^{27}Al\}$ and $^{17}O\{^{31}P\}$ REDOR experiments. Figure 2 illustrates a typical set of $^{17}O\{^{27}Al\}$ REDOR data including the ^{17}O spin−echo (S_0), REDOR (S), and REDOR difference (ΔS) spectra. Some information for spectral assignment can be extracted from the normal ^{17}O spin−echo spectrum of the control experiment (Figure 2A) alone since the spin−echo discriminates against the resonance with short spin−spin relaxation time (T_2). An inspection of the normal ^{17}O spin−echo spectrum (Figure 2A) reveals that compared to the simple ^{17}O MAS spectrum (Figure 1B) the intensity of the very broad component centered at around −40 ppm decreased significantly relative to the peak at +72 ppm. This spin−echo spectrum clearly indicates that the broad resonances at around −40 ppm and the maximum at ca. +34 ppm belong to different sites. The corresponding REDOR difference spectrum (Figure 2C) contains only two overlapping resonances near +70 ppm, which can be closely simulated by using two second-order quadrupolar line-shapes (Figure 2D). Observing these signals in the $^{17}O\{^{27}Al\}$ REDOR difference spectrum indicates unambiguously that these two ^{17}O sites are bonded to Al. The very broad component at high field centered at around −40 ppm, on the other hand, did not appear in the REDOR difference spectrum, suggesting that this oxygen is not connected to Al. The $^{17}O\{^{27}Al\}$ REDOR data suggest that there are three distinct ^{17}O chemical environments. Using the REDOR results, the ^{17}O MAS spectrum was simulated with three sites (Figure 3) by using the quadrupolar coupling constant (C_q), asymmetry parameter (η), and isotropic chemical shift (δ_{iso}) of the two low-field resonances estimated from the REDOR experiments as initial values.

The 80-min sample also contains a small amount of unreacted alumina as indicated by the ^{27}Al MAS spectrum (Supporting Information Figure S1). The ^{27}Al MAS spectra of 0, 30, 80, and 160 min samples all contain three peaks. The peaks at +45 and −5 ppm are due to tetrahedral and octahedral Al sites in the AlPO phases, respectively. The peak at +9 ppm was previously assigned to the unreacted alumina.[21] Since their line-shapes and quadrupolar parameters (Table 1) are very similar to those in Al_2O_3 reported in the literature,[22] the two low-field resonances in the ^{17}O MAS spectrum are assigned to the $^{17}O(-Al)_4$ and $^{17}O(-Al)_3$ environments in unreacted alumina.

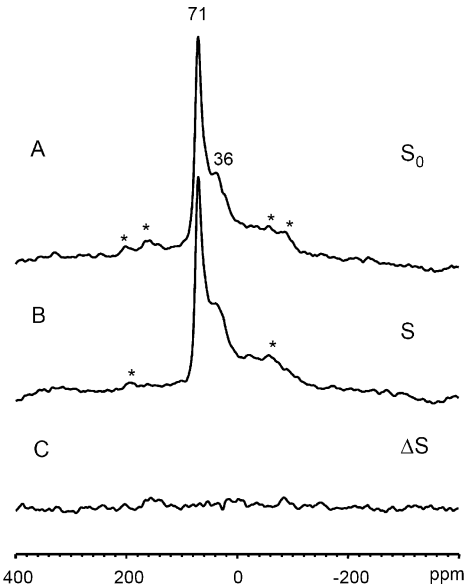

Figure 4. $^{17}O\{^{31}P\}$ REDOR spectra of 80-min dry-gel sample (four rotor periods were applied at 7 kHz ± 2 Hz). A total of 79,000 scans were acquired with a recycle time of 0.5 s. The total experimental time was 22 h. (A) ^{17}O spin−echo (S_0); (B) REDOR (S); and (C) REDOR difference (ΔS) spectra. Asterisks indicate spinning sidebands.

To confirm these assignments, we further carried out the $^{17}O\{^{31}P\}$ REDOR experiments. No signal was observed in $^{17}O\{^{31}P\}$ REDOR difference spectrum (Figure 4), demonstrating that none of the ^{17}O signals seen in the MAS spectrum is coupled to P. Thus, the $^{17}O\{^{31}P\}$ REDOR results are supportive of the assignments for the two low-field resonances observed in the $^{17}O\{^{27}Al\}$ REDOR difference spectrum. Since the broad high-field resonance at around −40 ppm seen in the ^{17}O MAS spectrum did not show up in either $^{17}O\{^{27}Al\}$ or $^{17}O\{^{31}P\}$ REDOR difference spectrum, we assign this broad signal to the water molecules bound to the solids with restricted mobility. $^1H \rightarrow {}^{17}O$ cross polarization spectrum with a short contact time (Figure 5) shows a broad asymmetric peak. The broad profile likely contains contributions from $H-{}^{17}O(-Al)_3$ and the water molecules strongly bonded to the solids. The sharp low-field resonance at +72 ppm observed in the MAS spectrum did not appear in the CP spectrum, which is in agreement with the $^{17}O(-Al)_4$ environment.

The ^{17}O NMR results indicate that, after treating the initial dry-gel for 80 min, ^{17}O-enriched water starts penetrating into the solids and replacing the water molecules initially occluded

(21) Huang, Y.; Richer, R.; Kirby, C. W. *J. Phys. Chem. B* **2003**, *107*, 1326−1337.
(22) Walter, T. H.; Oldfield, E. *J. Phys. Chem.* **1989**, *93*, 6744−6751.

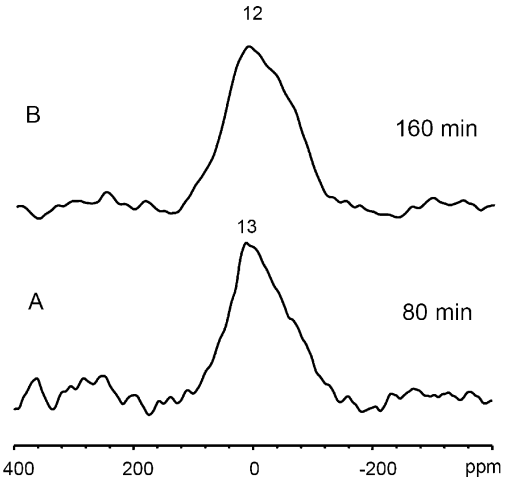

Figure 5. $^{1}H \rightarrow {}^{17}O$ CP MAS spectra of selected dry-gel samples with a contact time of 80 μs. (A) 80-min sample: the spinning rate was 12 kHz. A total of 23,776 scans were acquired with a recycle time of 5 s. The total experimental time was 33 h. (B) 160-min sample: the spinning rate was 10 kHz. A total of 19,172 scans were acquired with a recycle time of 5 s. The total experimental time was 26.6 h.

in the dry-gel powder. The ^{17}O-enriched water from vapor phase reacts first with alumina. Neither cleavage of the Al−O−P linkage nor oxygen exchange at the P−O−H group in the layered material has taken place at this stage.

The overall appearance of the ^{17}O MAS spectrum of the 160-min sample (Figure 1B) looks somewhat similar to that of the 80-min sample except that, in addition to the sharp peak at +72 ppm, there are two well-defined maxima at +33 and −31 ppm superimposed on a very broad envelope. Relative to the sharp peak at +72 ppm, the intensities of the broad overlapping resonances are stronger than those of the 80-min sample, suggesting that more ^{17}O atoms have been incorporated into the solid species. The poor resolution of the MAS spectrum, however, prevents us from directly extracting structural information. Again, $^{17}O/^{27}Al$ and $^{17}O/^{31}P$ double-resonance experiments were performed to assist in the detailed spectral assignments. The simulation of the $^{17}O\{^{27}Al\}$ REDOR difference spectrum (Figure 6) shows that the overlapping center bands consist of three ^{17}O signals that are coupled to Al. In addition to the $^{17}O(-Al)_4$ and $^{17}O(-Al)_3$ sites in unreacted alumina seen in the 80-min sample, there is a new component with a well-defined second-order quadrupolar line-shape. The line-shape and its ^{17}O quadrupolar parameters estimated from the simulation (Figure 6) are similar to those of oxygen in Al−O−P linkage in $AlPO_4$-based molecular sieves.[10b] Therefore, we assign this new resonance to the oxygen in an $Al-{}^{17}O-P$ unit. Two overlapping signals were observed in the $^{17}O\{^{31}P\}$ REDOR difference spectrum (Figure 7). One component is due to the oxygen site in $Al-{}^{17}O-P$ linkage since its ^{17}O quadrupolar parameters are almost identical to those obtained from the $^{17}O\{^{27}Al\}$ REDOR experiments (Figure 6). The second resonance is assigned to the $P-{}^{17}O-H$ group as the isotropic chemical shift and quadrupolar coupling parameters obtained from the simulation of the spectrum (Figure 7) are comparable to those reported for $P-{}^{17}O-H$ groups in various phosphates.[23] $^{1}H \rightarrow {}^{17}O$ CP spectrum of the 160-min sample is shown in Figure 5B. Although the very broad profile is somewhat similar

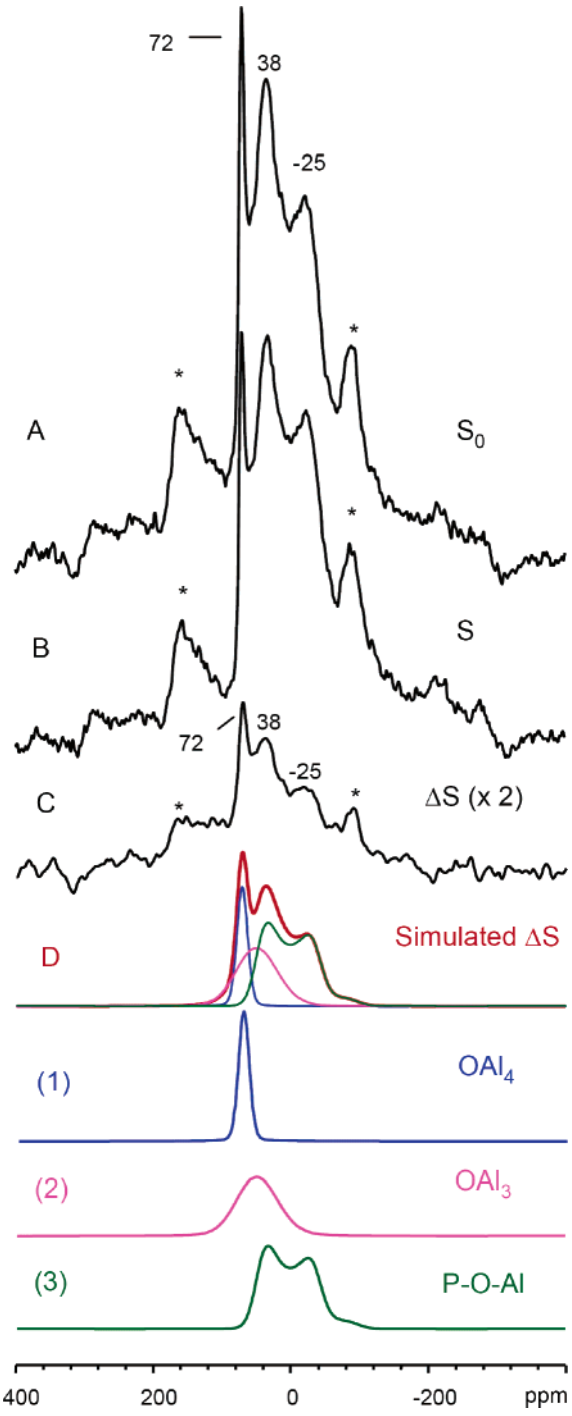

Figure 6. $^{17}O\{^{27}Al\}$ REDOR spectra of the dry-gel sample heated for 160 min. Ten rotor cycle periods were applied with a spinning rate at 7 kHz ± 2 Hz. A total of 92,000 scans were acquired with a recycle time of 0.5 s. The total experimental time was 25.6 h. (A) ^{17}O spin−echo (S_0); (B) REDOR (S); and (C) REDOR difference (ΔS) spectra. Asterisks indicate spinning sidebands. (D) Simulated REDOR difference spectrum using three components in a 1:1.5:2.5 ratio: (1) $C_q = 1.3$ MHz, $\eta = 0$, $\delta_{iso} = 74$ ppm, 840 Hz line broadening. (2) $C_q = 4.0$ MHz, $\eta = 0$, $\delta_{iso} = 74$ ppm, 1120 Hz line broadening. (3) $C_q = 5.7$ MHz, $\eta = 0$, $\delta_{iso} = 68$ ppm, 558 Hz line broadening.

to that of the 80-min sample (Figure 5A), it now has an additional contribution from $P-{}^{17}O-H$ groups.

The ^{17}O MAS spectrum of the 160-min sample was then simulated to obtain more accurate quadrupolar parameters (Figure 8). The C_q, η, and δ_{iso} values for four sites obtained

(23) Wu, G.; Rovnyak, D.; Huang, P. C.; Griffin, R. G. *Chem. Phys. Lett.* **1997**, *277*, 79−83.

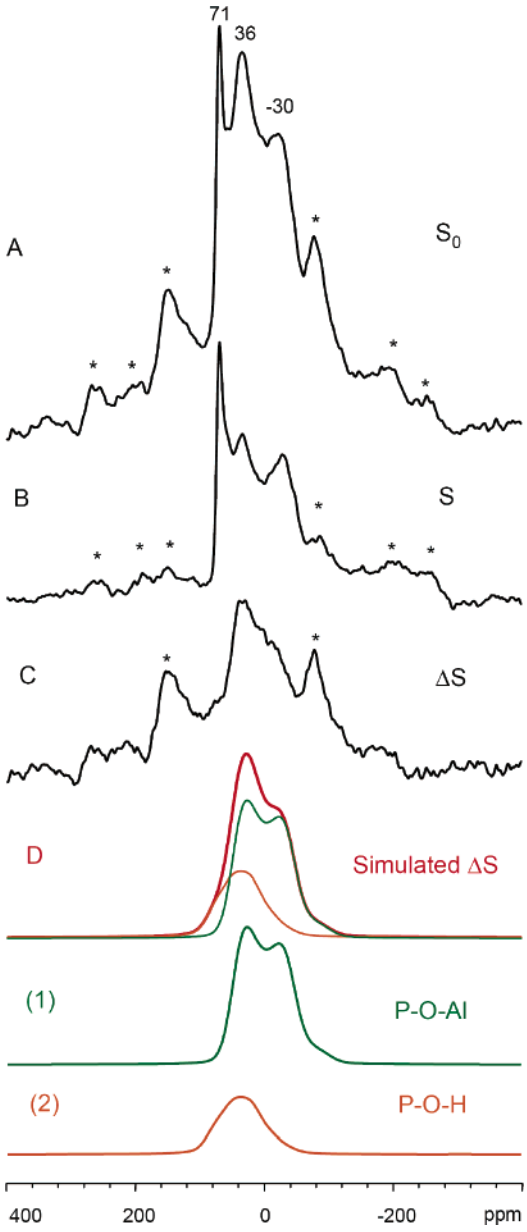

Figure 7. $^{17}O\{^{31}P\}$ REDOR spectra of 160-min dry-gel sample (10 rotor periods were applied at 6.5 kHz ± 2 Hz). A total of 65,908 scans were acquired with a recycle time of 0.5 s. The total experimental time was 19 h. (A) ^{17}O spin−echo (S_0); (B) REDOR (S); and (C) REDOR difference (ΔS) spectra. Asterisks indicate spinning sidebands. (D) Simulated REDOR difference spectrum using two components in a 2.3:1 ratio: (1) $C_q = 5.7$ MHz, $\eta = 0$, $\delta_{iso} = 65$ ppm, 2500 Hz line broadening. (2) $C_q = 5.1$ MHz, $\eta = 0.55$, $\delta_{iso} = 95$ ppm, 2400 Hz line broadening.

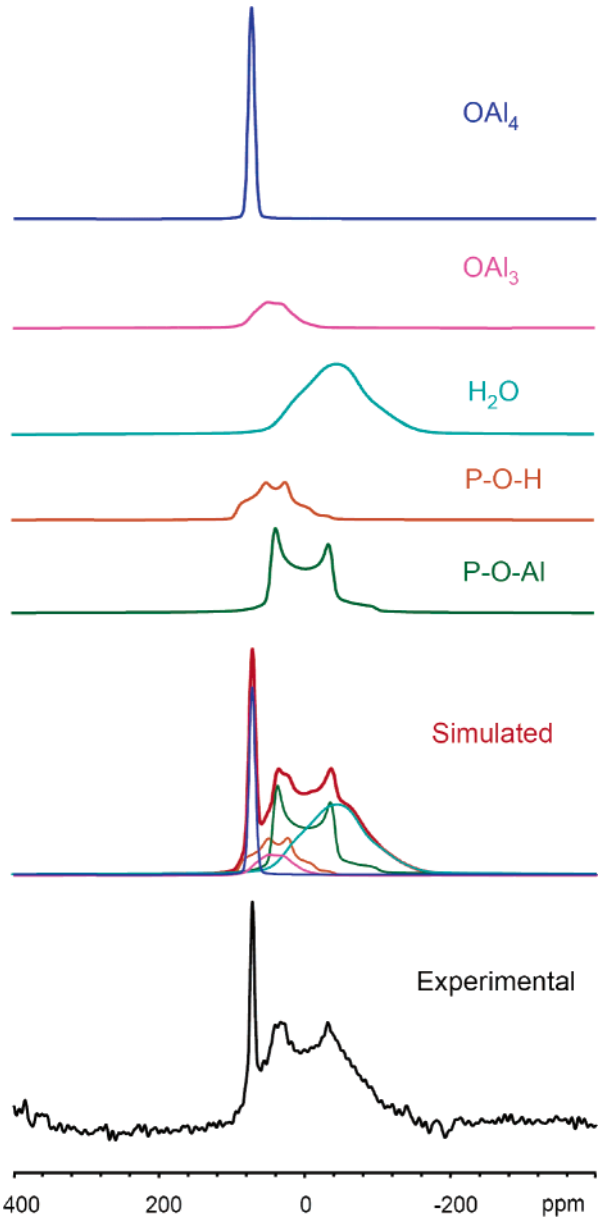

Figure 8. Simulation of ^{17}O MAS NMR spectrum of 160-min dry-gel sample. The quadrupolar parameters used for fitting the data are listed in Table 1.

from fitting REDOR difference spectra can only be used as initial values for fitting MAS spectrum because the spinning speeds used in the REDOR experiments were low, resulting in the center bands overlapping partially with the sidebands. Further, the different sites may have different T_2 relaxation times. The simulated ^{17}O MAS spectrum of the 160-min sample reveals that there are five different oxygen sites: $^{17}O(-Al)_4$, $^{17}O(-Al)_3$, Al−^{17}O−P, P−^{17}O−H, and $H_2{}^{17}O$ and the corresponding C_q, η, and δ_{iso} values are listed in Table 1. The ^{17}O NMR results show that after heating the dry-gel for 160 min, a significant number of oxygen atoms in P−O−H groups in the layered material have exchanged with the ^{17}O atom from water vapor. ^{17}O atoms have also been incorporated into the Al−O−P linkage, but it is not clear whether the Al−^{17}O−P linkage is in the layered intermediate or in the framework of $AlPO_4$-11 since the ^{17}O line-shapes of Al−O−P unit in layered phase and $AlPO_4$-11 are likely very similar.

To clarify the situation, we acquired the $^{17}O \rightarrow {}^{31}P$ CP spectrum (Figure 9B), which illustrates a strong peak at −18 and a broad weak resonance at −25 ppm. We have assigned the −18 ppm peak in corresponding ^{31}P MAS spectrum (Figure 9C) to the P site in the layered phase with a (H−O)−P−(O−Al)$_3$ environment.[20] Observing this peak with strong intensity in the $^{17}O \rightarrow {}^{31}P$ CP spectrum suggests that most Al−O−P units containing ^{17}O atoms are in the layered material. Apparently, a significant amount of ^{17}O atoms have been incorporated in both P−O−H and Al−O−P units in (H−O)−P−(O−Al)$_3$ of the layered phase.

As illustrated in Scheme 3A, $AlPO_4$-11 has three crystallographically nonequivalent P sites[24] that manifest themselves in

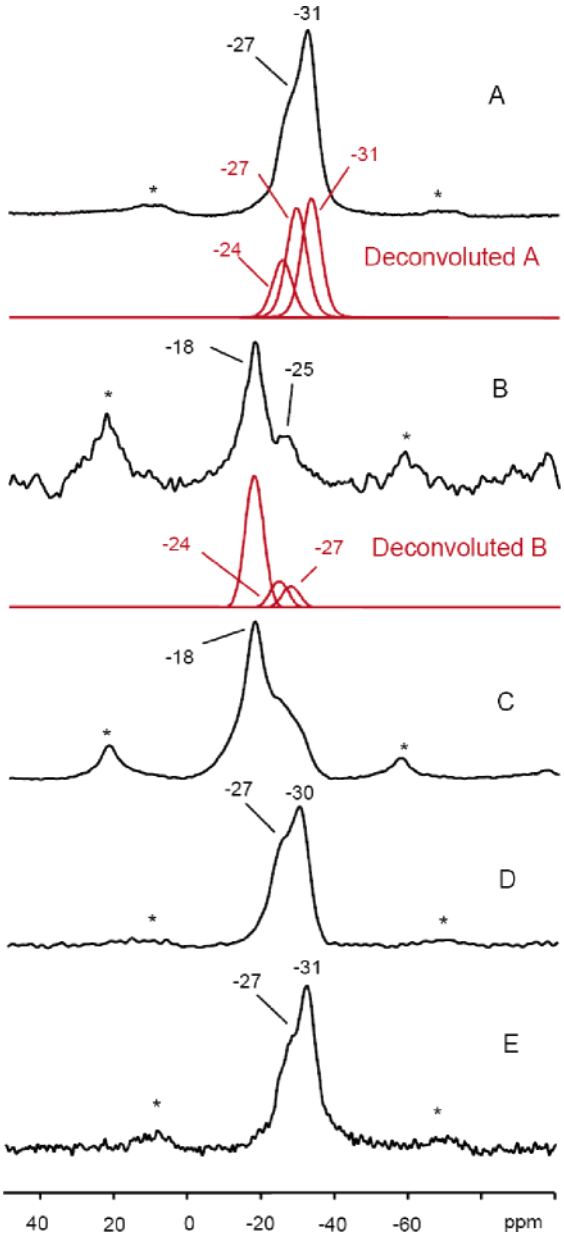

Figure 9. (A) Experimental and deconvoluted spectra of ^{31}P MAS spectra of as-made $AlPO_4$-11 (72 h sample). (B) $^{17}O \rightarrow {}^{31}P$ CP MAS experimental and deconvoluted spectra of 160-min dry-gel sample. The contact time was 1 ms. The spinning rate was 6.5 kHz. A total of 160,000 scans were acquired with a recycle time of 0.5 s. The total experimental time was 22.2 h. (C) ^{31}P MAS spectrum of the 160-min dry-gel sample; (D) $^{1}H \rightarrow {}^{31}P$ CP MAS spectrum of the 160-min dry-gel sample with a contact time of 80 ms. (E) $^{17}O \rightarrow {}^{31}P$ CP MAS spectrum of as-made $AlPO_4$-11 (72 h sample). The contact time was 1 ms. The spinning rate was 6.5 kHz. A total of 160,000 scans were acquired with a recycle time of 0.5 s. Asterisks indicate spinning sidebands.

the ^{31}P MAS spectrum as a broad asymmetrical peak. The deconvoluted spectrum exhibits three resonances at −24, −27, and −31 ppm with an intensity ratio 1:2:2 (Figure 9A). In the literature, the −24 ppm resonance has been assigned to the P(3) sites in the junction of the six- and six-membered rings.[25] The assignments for −27 and −31 ppm peak, however, are not

Scheme 3. (A) Projection of $AlPO_4$-11 Structure along [001] Direction with Three Crystallographically Nonequivalent P Sites Shown and (B) Illustration of the Interaction between Protonated DPA and the Oxygen Atoms Bonded to the P at the Junction of Four- and Six-Membered Ring (see text)

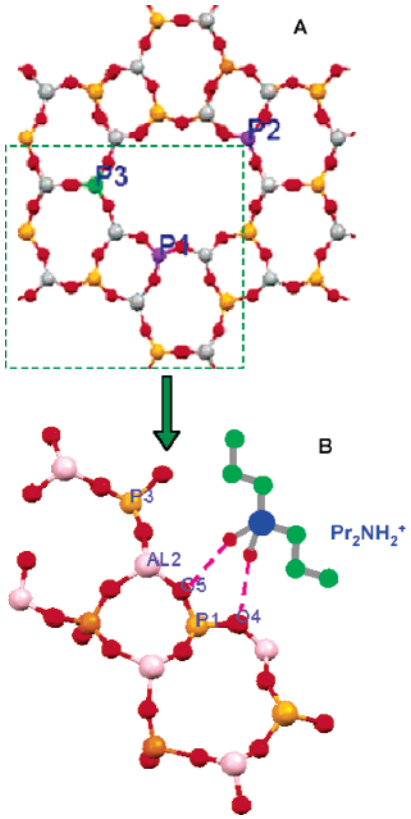

possible because both P(1) and P(2) are in the junction of the six- and four-membered rings with the same site occupancy. The ^{31}P MAS spectrum of 160-min sample (Figure 9C) shows a broad shoulder on the high-field side of the −18 ppm peak. Observing this shoulder with the breadth from −24 to −30 ppm is consistent with the corresponding XRD pattern, showing that a noticeable amount of $AlPO_4$-11 has formed (Figure 1A). However, from the ^{31}P MAS spectrum alone it is not clear if all three P sites were fully developed. The $^{1}H \rightarrow {}^{31}P$ CP was used to select P signals of $AlPO_4$-11 since the proton spin−lattice relaxation time in rotating frame of reference ($T_{1\rho}{}^{H}$) for $AlPO_4$-11 is long.[21] The long $T_{1\rho}{}^{H}$ should discriminate in favor of the P signals of $AlPO_4$-11. Indeed, the $^{1}H \rightarrow {}^{31}P$ CP spectrum with a long contact time of 80 ms exhibits only the P signals from $AlPO_4$-11 (Figure 9D). The correct intensity ratio suggests that all three P sites are fully developed. Interestingly, the deconvoluted $^{17}O \rightarrow {}^{31}P$ CP spectrum (Figure 9B) exhibits only two weak peaks at −24 and −27 ppm. Observation of the signals belonging to $AlPO_4$-11 in $^{17}O \rightarrow {}^{31}P$ CP spectrum suggests that ^{17}O-labeled water is directly involved in the transformation of the layered phase to $AlPO_4$-11 and that a small portion of the Al−^{17}O−P linkages seen in the $^{17}O\{^{31}P\}$ REDOR difference spectrum must originate from Al−^{17}O−P in $AlPO_4$-11. The fact that the −31 ppm peak does not appear in the $^{17}O \rightarrow {}^{31}P$ CP spectrum indicates that no ^{17}O atom has entered the first coordination sphere of this particular P site upon the formation of $AlPO_4$-11. Previous studies have shown that there is a strong hydrogen bonding between two oxygen atoms

(24) Richardson, J. W., Jr.; Pluth, J. J.; Smith, J. V. *Acta Crystallogr.* **1988**, B44, 367−373.
(25) (a) Tapp, N. J.; Milestone, N. B.; Bowden, M. E.; Meinhold, R. H. *Zeolites* **1990**, *10*, 105−110. (b) Barrie, P. J.; Smith, M. E.; Klinowski, J. *Chem. Phys. Lett.* **1991**, *180*, 6−12.

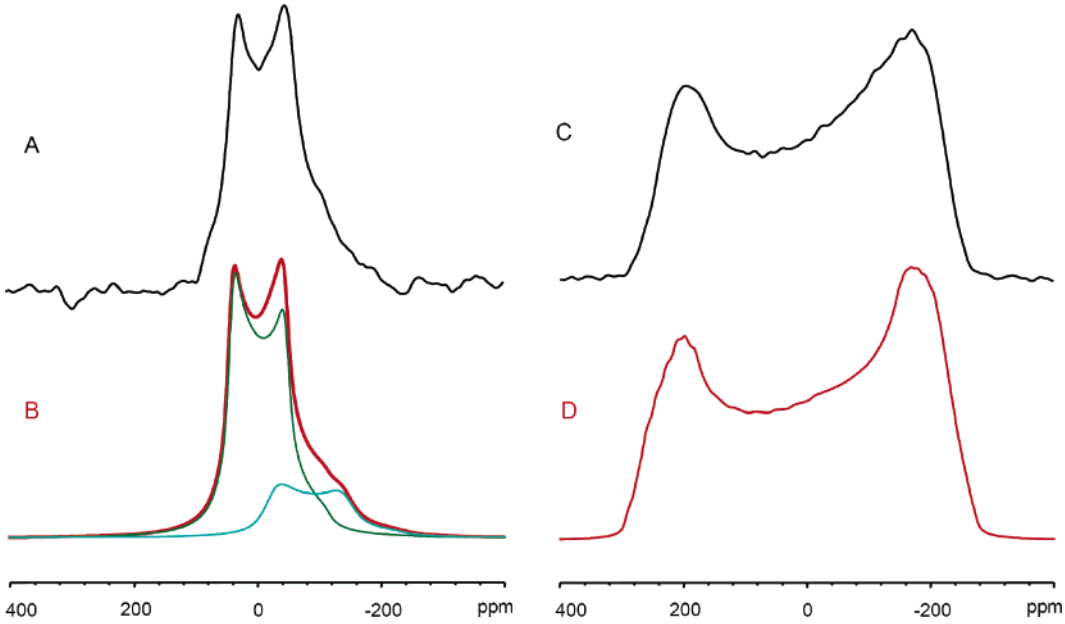

Figure 10. ^{17}O MAS NMR spectra of as-made $AlPO_4$-11 (72 h sample): (A) experimental spectrum and (B) simulated spectrum. ^{17}O static spectra of as-made $AlPO_4$-11 (72 h sample): (C) experimental spin−echo spectrum and (D) simulated static spectrum. The quadrupolar parameters used for fitting the data are listed in Table 1.

[O(4) and O(5)] that are directly bound to P(1) site and the two hydrogen atoms attached to the N atom in the protonated SDA in as-made $AlPO_4$-11.[26] The absence of the −31 ppm peak in the $^{17}O \rightarrow {}^{31}P$ CP spectrum suggests that the same unit involving a pair of adjacent four- and six-membered rings interacting with a protonated DPA molecule via hydrogen bonding also exists in the layered phase. Apparently, this unit remains unaffected upon transformation to $AlPO_4$-11, and it is the P at the junction of the four- and six-membered rings that evolves to become the P(1) site in $AlPO_4$-11. The H-bonding prevents the ^{17}O isotopic exchange from occurring at this particular site (Scheme 3B). As mentioned earlier, the two peaks at −27 and −31 ppm in the ^{31}P MAS spectrum of $AlPO_4$-11 cannot be assigned to P(1) or P(2). Since only P(1) is involved in H-bonding with SDA,[26] we are now able to assign the peaks at −31 and −27 ppm to P(1) and P(2), respectively, based upon the $^{17}O \rightarrow {}^{31}P$ CP spectrum.

The ^{17}O MAS spectrum of highly crystalline $AlPO_4$-11 obtained by heating the initial dry-gel for 72 h is shown in Figure 10A and the simulated MAS spectrum reveals two resonances due to the oxygen in Al−O−P and water occluded in the framework. The ^{17}O nuclear quadrupolar parameters (C_q, η) extracted from the simulated MAS and static spectra (Figure 10) are comparable to those of $AlPO_4$-11 reported previously.[10b] The overall appearance of the $^{17}O \rightarrow {}^{31}P$ CP spectrum (Figure 9E) of as-made $AlPO_4$-11 looks very similar to that of the corresponding ^{31}P MAS spectrum (Figure 9A), suggesting that heating the dry-gel for a sufficiently long time under SAC conditions leads to ^{17}O isotopic exchange that eventually occurs at all the oxygen sites in the framework. It is also noted that the ^{17}O signals due to alumina gradually decreased and eventually disappeared with increasing the heating time (Figure 1B). This suggests that there might be a small amount of phosphate-based domain in the dry-gel powder that reacts with alumina to form AlPO-based intermediate and eventually $AlPO_4$-11.

Summary

The present work provides unambiguous evidence for the direct involvement of ^{17}O-enriched water vapor during the crystallization of molecular sieves by the DGC method. For $AlPO_4$-11, the first 30 min of heating under SAC conditions does not lead to incorporation of ^{17}O atom into any solid species. Heating the initial dry-gel powder for 80 min results in the ^{17}O-enriched water from vapor slowly exchanging with $H_2{}^{16}O$ molecules tightly adsorbed in the initial dry-gel. $H_2{}^{17}O$ reacts with a small amount of alumina in the dry-gel powder first before hydrolyzing the Al−O−P linkage in the AlPO-based intermediates. After 160-min heating, bond breaking and reforming occur at both P−O−H and Al−O−P units of the layered phase. Interestingly, during nucleation, ^{17}O atoms are preferably bonded only to the P(2) and P(3) sites in $AlPO_4$-11. The ^{17}O exchange does not occur at the P(1) site due to the H-bonding of protonated DPA with the oxygen atoms in the first coordination sphere of this P. The implication is that the joint four- and six-membered rings may already exist in the layered phase and remain unaffected upon transformation into $AlPO_4$-11, which is consistent with the absence of the peak at −31 ppm due to this P in the $^{17}O \rightarrow {}^{31}P$ CP spectrum. This selectivity is a kinetic phenomenon, since after an extended heating period ^{17}O atoms are evenly distributed throughout the framework.

This work demonstrates that ^{17}O NMR is a sensitive technique for monitoring the role of water in the formation of molecular sieves by dry-gel conversion methods. It can be foreseen that this approach may have applicability in examining the crystallization kinetics and mechanisms of zeolites and other related materials using DGC methods. Experiments of this type are

(26) (a) Prasad, S.; Vetrivel, R. *J. Phys. Chem.* **1992**, *96*. 3092−3096. (b) Pluth, J. J.; Smith, J. V.; Richardson, J. W., Jr. *J. Phys. Chem.* **1988**, *92*, 2734−2738.

currently in progress in our lab using the general approach described in this article.

Acknowledgment. Y.H. thanks the Natural Science and Engineering Research Council of Canada for a research grant and the Canada Foundation for Innovation for the award of a 400 MHz solid-state NMR spectrometer. Funding from the Canada Research Chair and Premier's Research Excellence Award programs is also gratefully acknowledged. We thank Prof. R. E. Wasylishen for kindly providing the software WSOLIDS and Dr. C. Kirby for technical assistance.

Supporting Information Available: Additional experimental results (1 figure). This material is available free of charge via the Internet at http://pubs.acs.org.

JA060286T